pulse. For large values of $[I/I_c-1]$, the growth of the normal phase over the length of the specimen becomes too fast to observe. This is probably the result of the formation of many normal bridges plus a very large velocity of normal phase propagation. Thus, the specimen, which has a pulse-transmission coefficient typically in the range of 30 to 60% when normal, effectively clips the incident pulse "long" before it reaches full amplitude. Although the rise time of the incident pulse is about 3×10^{-10} sec, transmitted-pulse rise times have been measured in the range $1.0-1.1\times10^{-10}$ sec. Since the rise time of this particular oscilloscope has been measured by the manufacturer to be 9.5×10^{-11} sec, values of τ less than 5×10^{-11} sec are indicated. This follows if one makes the usual assumption that the square of the rise time of the observed pulse is the sum of the squares of the actual-pulse rise time and that of the oscilloscope.

Therefore, we must conclude that, in the limit of large values of (I/I_c-1), the time required to create a primordial normal nucleus is not more than 5×10^{-11} sec and perhaps considerably less.

We would like to thank Dr. B. Rosenblum and Dr. W. H. Cherry for many helpful discussions.

The authors would like to note that since this paper was submitted for publication, other pulse measurements have been reported[8] which also indicate switching times of the order of tens of picoseconds or less.

[8] F. B. Hagedorn, Phys. Rev. Letters **12**, 322 (1964).

PHYSICAL REVIEW VOLUME 135, NUMBER 2A 20 JULY 1964

Bulk Absorption of Radiation in Superconductors†

ERNEST E. H. SHIN
National Magnet Laboratory, Massachusetts Institute of Technology, Cambridge, Massachusetts*
(Received 11 February 1963; revised manuscript received 27 February 1964)

Perturbation theory is applied to calculate the spectral shape of the bulk absorption of radiation in a superconductor. The second-order processes involving one photon and one phonon are considered. The resulting spectrum exhibits a spike near the frequency corresponding to the energy gap. This is attributed to the large values of the BCS density of states at the gap edges.

I. INTRODUCTION

IT has been shown that the bulk absorption due to the second-order processes, each involving one photon and one phonon, contribute significantly to the infrared absorption of normal metals at very low temperatures.[1-3] That the contribution of these processes may be significant in a superconductor which has large electron-phonon interaction has been pointed out by Richards and Tinkham.[4] While calculations on both the bulk radiative[5] and nonradiative[6] recombination rates and of the absorption associated with the anomalous skin effects[7,8] have been offered previously, similar studies on the bulk absorption processes (unpairing) have not been reported.

In the present paper, the bulk absorption rate is calculated as a function of the radiation frequency. As a result, it is shown that the absorption spectrum exhibits a spike (i.e., a maximum) near the gap frequency. The previous calculations of the *skin* absorption by Mattis and Bardeen[7] and Miller[8] do not exhibit such a structure.

The subject matter is of considerable current interest in view of the suggestion, made by Burstein *et al.*[5] on possible use of a superconducting sandwich of metals as a radiation detector, and particularly in view of the recent experimental development in this direction reported by Dayem and Martin.[9] The observations by Dayem and Martin on a superconducting sandwich composed of two superconducting metals and a dielectric layer between them, indicate that, upon absorption of radiation quanta, the paired electrons in one metal are unpaired, being taken, across the barrier, to the unpaired band of the other metal. This, admittedly, is not quite the same as what happens in an absorptive unpairing in a single superconducting metal. The physical explanation for the absorptive tunneling processes, however, is yet unavailable. It is hoped, therefore, that the calculations presented here on a single supercon-

* Operated with support by the U. S. Air Force Office of Scientific Research.

† A part of this work was conducted at Parametrics, Inc.

[1] T. Holstein, Phys. Rev. **96**, 535 (1954).

[2] M. Biondi, Phys. Rev. **102**, 964 (1956).

[3] R. N. Gurzhi, Zh. Eksperim. i Teor. Fiz. **33**, 451, 660 (1957); **35**, 965 (1958) [English transls.: Soviet Phys.—JETP **6**, 352, 506 (1958); **8**, 673 (1959)].

[4] P. L. Richards and M. Tinkham, Phys. Rev. **119**, 575 (1960).

[5] E. Burstein, D. Langenberg, and B. Taylor, Phys. Rev. Letters **6**, 92 (1961).

[6] J. R. Schrieffer and D. M. Ginsberg, Phys. Rev. Letters **8**, 207 (1962).

[7] D. C. Mattis and J. Bardeen, Phys. Rev. **111**, 412 (1958).

[8] P. B. Miller, Phys. Rev. **118**, 928 (1960).

[9] A. H. Dayem and R. J. Martin, Phys. Rev. Letters **8**, 246 (1962).

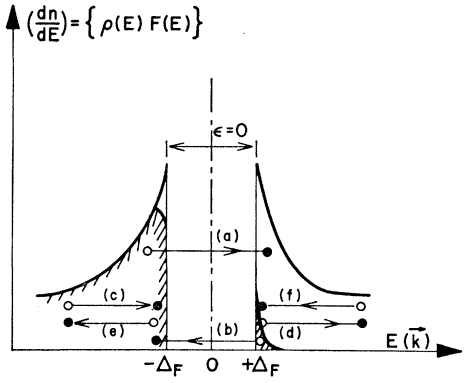

FIG. 1. Schematic illustration of the paired and the unpaired population distributions, and various competing processes of absorption (a,c,d) and emission (b,e,f) in a superconductor.

ductor may be of pertinence to further studies on the problem.

The absorption of superconductors has been observed by Richards and Tinkham[4] and more recently by Richards.[10] In fact, the earlier absorption spectrum observed by Richards and Tinkham exhibited a structure which is indicative of the spike such as what results in the present calculations and the later observations by Richards,[10] also suggest a structure similar to what has been obtained here.[11]

It is pointed out, further, that the over-all shape of the absorption spectrum, as well as the spike of the present calculations, bear resemblance with the current-voltage characteristics curves of a superconducting sandwich of metals,[12] the spike of the absorption spectrum corresponding to the negative resistance region of the sandwich. The spike of the sandwich is known to be due to the high density of states at the gap edges.[12] The same explanation is given for the spike of the absorption spectrum in consideration here.

II. COMMENTS ON VARIOUS COMPETING BULK PROCESSES

In a superconductor interacting with an external radiation field, various competing processes of absorption and emission can take place. In particular, the absorption may take place either across the energy gap, within the unpaired band, or within the paired band. Different processes of bulk absorption and emission are shown in Fig. 1, where the population distributions of the paired and unpaired electrons are also shown.

Before proceeding to the calculations on the bulk absorptive unpairing processes, therefore, it seems pertinent to show first that other possible processes of absorption contribute little to the over-all absorption compared with the intergap transitions.

For an absorption or emission transition from the initial state of energy E_i to the final state of energy E_f, the rate of the process w_{if} is proportional to

$$\{\rho(E_i)\rho(E_f)F(E_i)[1-F(E_f)]\}\,, \tag{1}$$

$$\rho(E)\cong N(0)\left|\frac{E}{(E^2-\Delta_F{}^2)^{1/2}}\right|\,, \quad |E|>\Delta_F\,,$$
$$=0\,, \qquad\qquad |E|<\Delta_F\,; \tag{2}$$

$$F(E)=1/(1+e^{\beta E})\,,$$
$$E=(\epsilon^2+\Delta_F{}^2)^{1/2}\,, \tag{3}$$

where $\beta=(k_\beta T)^{-1}$, ϵ is the Bloch single-particle energy relative to the Fermi energy E_F, and Δ_F is $\frac{1}{2}$ the energy gap at the Fermi level.

If the absorbed or emitted quantum $\hbar\omega$ is equal to or only slightly larger than $2\Delta_F$, and $(E_f-E_i)\approx\pm\hbar\omega$, the formula (1) leads to the following relations among the rates $w_{if}{}^{(a)}-w_{if}{}^{(f)}$;

$$\frac{w_{(c)}}{w_{(a)}}\cong\frac{w_{(d)}}{w_{(a)}}\cong\frac{w_{(e)}}{w_{(b)}}\cong\frac{w_{(f)}}{w_{(b)}}\cong O\left(\frac{1}{D_c}e^{-\beta\Delta_F}\right), \tag{4}$$

when $\beta\Delta_F\gg1$, where D_c is the cutoff value of the BCS[13] density-of-states function at $|E|=\Delta_F$,[14]

$$D_c=\{\rho(\Delta_F)/N(0)\}\,, \tag{5}$$

which is in general substantially larger than unity.

Similarly, it can be also shown that the emission rate $w_{(b)}$ is smaller than $w_{(a)}$ by a factor of $e^{-\beta\hbar\omega}$ when $\beta\hbar\omega\gg1$.

Thus, it is quite clear that only the process (a) is important when $\beta\Delta_F\gg1$; i.e., when temperature T is much lower than that representing the energy gap. The spectral shape that will be calculated in III for the process (a) will, therefore, represent very closely the over-all bulk absorption of a superconductor at very low temperatures.

III. INTERGAP ABSORPTION RATE

The bulk processes of the direct, first-order intraband absorption and emission are not possible for electrons in a metal since they cannot be made to meet the requirement for conservation of energy.[15] We shall therefore investigate the second-order processes illustrated by the Feynman diagrams in Fig. 2, where each diagram involves one photon and one phonon only.

If we write the interaction energy H_R, between electron and radiation, and H_P, between electron and phonon, as

$$H_R=H_R{}^{(+)}+H_R{}^{(-)}\,,$$
$$H_P=H_P{}^{(+)}+H_P{}^{(-)}\,, \tag{6}$$

[10] P. L. Richards, Phys. Rev. Letters **7**, 412 (1961).
[11] The author thanks Dr. Benjamin Lax for bringing this to his attention.
[12] See, for instance, S. Shapiro, P. A. Smith, J. Nicol, J. L. Miles, and P. F. Strong, IBM J. Res. Develop. **6**, 34 (1962).
[13] J. Bardeen, L. N. Cooper, and J. R. Schrieffer, Phys. Rev. **108**, 1175 (1957).
[14] A discussion on the significance of the cutoff parameter is given by L. C. Hebel, Phys. Rev. **116**, 79 (1959).
[15] See, for instance, H. J. G. Meyer, Phys. Rev. **112**, 298 (1958).

TABLE I. The energies of the initial, final, and intermediate states, denoted respectively by $\mathcal{E}_i$, $\mathcal{E}_f$, and $\mathcal{E}_B$, are shown. The numbers 1–4 refer to the Feynman diagrams of Fig. 2.

	$\mathcal{E}_i$	$\mathcal{E}_f$	$\mathcal{E}_B$
1	$E_{\mathbf{k}_i}+\hbar\omega$	$E_{\mathbf{k}_i+\mathbf{p}}$	$E_{\mathbf{k}_f}+\hbar\omega_{\lambda\mathbf{q}}$
2	$E_{\mathbf{k}_i}+\hbar\omega$	$E_{\mathbf{k}_i-\mathbf{K}}+\hbar\omega_{\lambda\mathbf{q}}+\hbar\omega$	$E_{\mathbf{k}_f}+\hbar\omega_{\lambda\mathbf{q}}$
3	$E_{\mathbf{k}_i}+\hbar\omega+\hbar\omega_{\lambda\mathbf{q}}$	$E_{\mathbf{k}_i+\mathbf{K}}+\hbar\omega$	$E_{\mathbf{k}_f}$
4	$E_{\mathbf{k}_i}+\hbar\omega_{\lambda\mathbf{q}}$	$E_{\mathbf{k}_i+\mathbf{p}}+\hbar\omega_{\lambda\mathbf{q}}$	$E_{\mathbf{k}_f}$

where (+) and (−) denote the creation and annihilation, respectively, of a photon $\hbar\omega$ in the case of H_R and of a phonon $\hbar\omega_{\lambda\mathbf{q}}$ with polarization $\lambda(=1, 2, 3)$ and wave vector $\mathbf{q}$ in the case of H_P, the relevant non-vanishing matrix elements are obtained as follows[15]:

$$\langle \mathbf{k}_f, O_\mathbf{p}|H_R^{(-)}|\mathbf{k}_i, O_\mathbf{p}|\rangle = \left(\frac{e}{\hbar\omega V}\right)^{1/2} \hat{\mathbf{e}}\cdot\left(\frac{d\epsilon(\mathbf{k}_i)}{d\mathbf{k}_i}\right)\delta_{\mathbf{k}_f,\,\mathbf{k}_1+\mathbf{p}},$$

$$\langle \mathbf{k}_f, (N_{\lambda\mathbf{q}}+1)|H_P^{(+)}|\mathbf{k}_i, N_{\lambda\mathbf{q}}\rangle = i\left(\frac{\hbar}{2V\omega_{\lambda\mathbf{q}}}\right)^{1/2}(N_{\lambda\mathbf{q}}+1)^{1/2}U_\lambda^{(+)}(\mathbf{k}_f,\mathbf{k}_i)\delta_{\mathbf{k}_f\,\mathbf{k}_i-\mathbf{K}}, \quad (7)$$

$$\langle \mathbf{k}_f, (N_{\lambda\mathbf{q}}-1)|H_P^{(-)}|\mathbf{k}_i, N_{\lambda\mathbf{q}}\rangle = i\left(\frac{\hbar}{2V\omega_{\lambda\mathbf{q}}}\right)^{1/2}(N_{\lambda\mathbf{q}})^{1/2}U_\lambda^{(-)}(\mathbf{k}_f,\mathbf{k}_i)\delta_{\mathbf{k}_f\,\mathbf{k}_i+\mathbf{K}},$$

where various symbols are defined as $\mathbf{k}_i,\mathbf{k}_f$ = electron wave vectors, e = electron charge, V = sample volume, $\hat{\mathbf{e}}$ = unit vector in the direction of polarization of the radiation, $\mathbf{p}$ = wave vector of photon, $\mathbf{K}=\mathbf{q}+\mathbf{g}$, $\mathbf{g}$ = appropriate reciprocal lattice vector, $N_{\lambda\mathbf{q}}=1/(e^{\beta\hbar\omega_{\lambda\mathbf{q}}}-1)$, and $U_\lambda^{(\pm)}(\mathbf{k}_f,\mathbf{k}_i)$ is the electron-phonon matrix element for creation and annihilation of a phonon.[16]

The transition probability per unit time $w_{(a)}$ for the process (a) of Fig. 1 is found by the usual perturbation theory using the second-order matrix elements of the form

$$M_{(2)}^{(\pm)} = \left\{\frac{(f|H_R^{(-)}|B)(B|H_P^{(\pm)}|i)}{\mathcal{E}_i-\mathcal{E}_B} + \frac{(f|H_P^{(\pm)}|B')(B'|H_R^{(-)}|i)}{\mathcal{E}_i-\mathcal{E}_{B'}}\right\}, \quad (8)$$

where B and B' denote the intermediate states of energy $\mathcal{E}_B$ and $\mathcal{E}_{B'}$, and $\mathcal{E}_i$ denotes the energy of the initial states. The energies $\mathcal{E}_i$, $\mathcal{E}_B$, $\mathcal{E}_f$, $\mathcal{E}_B$, include the electron, photon and phonon energies all together. These energies for each of the four Feynman diagrams of Fig. 2 are tabulated in Table I. The over-all transition rate, in number of electrons per unit time, in the entire sample

[16] We adopt the same definition as in Ref. 6.

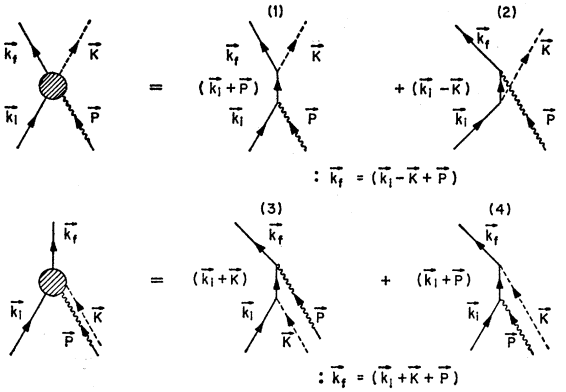

FIG. 2. The Feynman diagrams for the second-order absorption processes involving one photon and one phonon each. The solid, curved, and broken lines represent, respectively, the electron, photon, and phonon.

volume V may be found from the formula

$$P=\frac{2\pi}{\hbar}\sum_{(\pm)}\sum_{i,f}|M_{(2)}^{(\pm)}|^2F(E_i)\times[1-F(E_f)]|\mu_c|^2\delta(\mathcal{E}_i-\mathcal{E}_f), \quad (9)$$

where the electron energies E_i and E_f are to be distinguished from the energies $\mathcal{E}_i$ and $\mathcal{E}_f$, and the summation $(\pm)$ applies to the $(\pm)$ signs of the phonon. The quantity $|\mu_c|^2$ represents the coherence factor,

$$|\mu_c(\mathbf{k}_1,\mathbf{k}_2)|^2=\frac{1}{2}\left[1+\frac{\Delta_{\mathbf{k}_1}\Delta_{\mathbf{k}_2}-\epsilon_{\mathbf{k}_1}\epsilon_{\mathbf{k}_2}}{E_{\mathbf{k}_1}E_{\mathbf{k}_2}}\right]. \quad (10)$$

The rate P is defined in such a way as to include the temperature dependence and hence the statistical mechanical properties of the electrons.

Here we shall evaluate P for the simple case of a deformable ion model with spherical band structure. In this case, we simply have[6]

$$|U_\lambda^{(\pm)}(\mathbf{k}_f,\mathbf{k}_i)|^2\cong(C_\lambda^2q^2/\rho_M)(\mathbf{g}=0), \quad (11)$$

where C_λ is the Bloch interaction coefficient and ρ_M is the mass density of the lattice in grams per cm^3. For the present purpose, we may take $|\mu_c|^2\cong1$. This approximation is justified in view of the large values of the BCS density of states at the gap edges thus enabling the states at or near the Fermi level to participate more actively in the transitions than other states.

Upon using (7), (8), and (9), and after completing the usual algebraic steps, we obtain

$$P=\frac{2\pi}{\hbar}\left(\frac{\hbar e^2}{\omega\bar{V}}\right)\left(\frac{\hbar}{2\bar{V}\rho_M}\right)\left(\frac{\hbar}{m^*}\right)\left(\frac{1}{\hbar\omega}\right)^2\sum_\lambda\tfrac{1}{3}C_\lambda^2\frac{4V^2}{(2\pi)^6}\times\int\int\frac{dS_i}{\hbar v_i}\frac{dS_f}{dv_f}\int d\epsilon_i\int d\epsilon_f\left(\frac{q^4}{\omega_{\lambda\mathbf{q}}}\right)F(E_i)\times[1-F(E_f)]\{N_{\lambda\mathbf{q}}\delta(E_f-E_i-\hbar\omega_{\lambda\mathbf{q}}-\hbar\omega)+(N_{\lambda\mathbf{q}}+1)\delta(E_f-E_i+\hbar\omega_{\lambda\mathbf{q}}-\hbar\omega)\}, \quad (12)$$

where (dS_i) and (dS_f) represent elements of the energy surfaces at $\mathbf{k}_i$ and $\mathbf{k}_f$, and the integrals over ϵ_i and ϵ_f are to be carried over all possible range of the single-particle energy, and we have taken

$$\begin{aligned}&\hbar v_i=\left|\frac{d\epsilon_i}{d\mathbf{k}_i}\right|:\hbar v_f=\left|\frac{d\epsilon_f}{d\mathbf{k}_f}\right|,\\&(\mathbf{v}_f-\mathbf{v}_i)\cong\frac{\hbar(\mathbf{k}_f-\mathbf{k}_i)}{m^*}\cong\pm\frac{\hbar}{m^*}\mathbf{q}.\end{aligned}\tag{13}$$

In obtaining (12), we have explicitly used the energy values tabulated in Table I. We have dropped the photon wave vector $\mathbf{p}$ entirely since it merely constitutes a correction of the order of $(v/c)(\approx 10^{-2})$.[15]

The integrals over ϵ_i and ϵ_f can be converted to integrals over E_i and E_f upon using the relation,

$$d\epsilon=[\rho(E)/N(0)]dE:(|E|>\Delta_F)\,.\tag{14}$$

Henceforth, the vector sign of $\mathbf{q}$ will be dropped entirely due to the assumption of (11), and hence take

$$\omega_{\lambda\mathbf{q}}=\omega_{\lambda q}.$$

The surface integrals can be reduced to simpler form in the case of a spherical Fermi surface. We may thus use

$$\int\int\frac{dS_i dS_f}{\hbar^2 v_i v_f}\cdots=\frac{8\pi^2 k_F{}^2}{\hbar^2 v_F{}^2}\int_0^{q_D}q\,dq\cdots,\tag{15}$$

where q_D is the Debye cutoff, k_F is the magnitude of the wave vector at the Fermi level, and v_F is the magnitude of the Fermi velocity. Denoting the phase speed of sound for polarization λ by S_λ, we use the relations

$$\begin{aligned}&\hbar\omega_{\lambda q}=\hbar S_\lambda q,\\&k_B\theta_D{}^\lambda=\hbar S_\lambda q_D.\end{aligned}\tag{16}$$

The formula (12) is transformed into

$$\begin{aligned}P=&\frac{2\pi}{\hbar}\frac{4}{(2\pi)^6}\frac{8\pi^2}{3}\left(\frac{\hbar e^2}{\omega}\right)\left(\frac{\hbar}{2\rho_M}\right)\frac{k_F{}^2}{\hbar^7 m^{*2}\omega^2 v_F{}^2}\\&\times\sum_\lambda\frac{C_\lambda{}^2}{S_\lambda{}^6}\int_0^{Z_D}Z^4dZ\int_{-\infty}^{-\Delta_F}dE_i\int_{+\Delta_F}^{+\infty}dE_f\frac{\rho(E_i)\rho(E_f)}{[N(0)]^2}\\&\times F(E_i)[1-F(E_f)]\left\{\frac{1}{1-e^{-\beta Z}}\delta(E_f-E_i-Z-\hbar\omega)\right.\\&\left.+\frac{1}{e^{\beta Z}-1}\delta(E_f-E_i+Z-\hbar\omega)\right\},\end{aligned}\tag{17}$$

with $Z=\hbar\omega_{\lambda q}$, where the fact that the transitions take place from the paired band to the unpaired band has been made explicit by defining

$$\begin{aligned}&-\infty<E_i\leq-\Delta_F,\\&+\infty>E_f\geq+\Delta_F.\end{aligned}$$

Upon completing some further algebraic steps, (17) may be written in the form,

$$\begin{aligned}P=&\frac{1}{6\pi^3}\frac{e^2k_F{}^2}{\hbar^6 m^{*2}v_F\rho_M\omega^3}\sum_\lambda\frac{C_\lambda{}^2}{\beta^6 S_\lambda{}^6}\\&\times\left\{\int_{\alpha_1}^{x_D{}^\lambda}dx\frac{x^4\varphi(x)}{e^x-1}+\int_0^{\alpha_2}dx\frac{x^4\varphi(-x)}{1-e^{-x}}\right\},\end{aligned}\tag{18}$$

where

$$\begin{aligned}&\alpha_1=\quad 0\quad:\mu>2\beta\Delta_F\\&\quad=(2\beta\Delta_F-\mu):\mu<2\beta\Delta_F,\\&\alpha_2=\mu-2\beta\Delta_F:(x_D{}^\lambda+2\beta\Delta_F)>\mu>2\beta\Delta_F\\&\quad=\quad x_D{}^\lambda\quad:\quad\mu>(x_D{}^\lambda+2\beta\Delta_F),\\&\mu=\beta\hbar\omega:x=\beta\hbar\omega_{\lambda q},\\&\quad x_D{}^\lambda=\beta k_B\theta_D{}^\lambda,\end{aligned}$$

and

$$\begin{aligned}\varphi(x)=&\frac{1}{a}\left(\frac{a+b}{2}\right)^2\int_0^\pi d\theta\left(1-\left(\frac{2b}{a+b}\right)^2\cos^2\theta\right)\\&\times\left(1-\left(\frac{b}{a}\right)^2\cos^2\theta\right)^{1/2},\\a=&\left(\frac{x+\mu}{2}+\beta\Delta_F\right)\ (\geq 2\beta\Delta_F),\\b=&\left(\frac{x+\mu}{2}-\beta\Delta_F\right)\ (\geq 0).\end{aligned}\tag{19}$$

The integral $\varphi(x)$ may be solved by expanding the integrand in powers of $[(b/a)^2\cos^2\theta]$ since $(b/a)^2<1$. We can then write it in the form

$$\varphi(x)=\frac{2\pi}{2\beta\Delta_F+\mu+x}\left(\frac{\mu+x}{2}\right)^2 f(x),\tag{20}$$

where

$$\begin{aligned}f(x)=&\left\{1+\frac{1}{4}\left(\frac{y-2\beta\Delta_F}{y+2\beta\Delta_F}\right)^2-\frac{1}{2}\left(\frac{y-2\beta\Delta_F}{y}\right)^2\right.\\&+\frac{3}{16}\left(\frac{y-2\beta\Delta_F}{y+2\beta\Delta_F}\right)^2\left[\frac{3}{4}\left(\frac{y-2\beta\Delta_F}{y+2\beta\Delta_F}\right)^2\right.\\&\left.-\left(\frac{y-2\beta\Delta_F}{y}\right)^2\right]+\frac{5}{128}\left(\frac{y-2\beta\Delta_F}{y+2\beta\Delta_F}\right)^4\\&\times\left.\left[\frac{5}{2}\left(\frac{y-2\beta\Delta_F}{y+2\beta}\right)^2-3\left(\frac{y-2\beta\Delta_F}{y}\right)^2\right]+\cdots\right\}\\&:y=(x+\mu).\end{aligned}\tag{21}$$

A careful inspection of (21) reveals that $f(x)$ is of the

order of unity for all values of x that are involved in (18): at $y=2\beta\Delta_F$, $f=1$ and for $y\gg 2\beta\Delta_F$, $f\cong\frac{3}{4}$ so that f decreases monotomically from 1 to $\simeq\frac{3}{4}$ as y is increased from $2\beta\Delta_F$ to $+\infty$. This permits us to drop $f(x)$ entirely from $\varphi(x)$. The integrals of (18) can then be solved immediately.

While P represents the total rate of absorption in the sample volume V, it will be useful for practical purposes to define the absorption rates per unit volume per unit intensity of incident radiation (i.e., the absorption coefficient having the dimension of inverse length per unit energy of incident radiation) given by

$$A(\omega)=(P/I_0V)=(P/\hbar\omega c)\,, \tag{22}$$

where I_0 represents the intensity (in ergs/sec cm^2) of the incident radiation which is equal to $(\hbar\omega c/V)$ since we have adopted the convention of one quantum normalized in volume V.

Upon solving (18) as a function of ω, we obtain $A(\omega)$ for different ranges of ω as shown below.

(i) $\hbar\omega<2\Delta_F(\hbar\omega,\ 2\Delta_F\gg k_BT)$:

$$A(\omega)=\frac{2}{\pi^2}\left(\frac{e^2}{\hbar c}\right)\frac{k_F{}^2\Delta_F}{\hbar^2m^{*2}v_F{}^2\rho_M}\left(\sum_\lambda\frac{C_\lambda{}^2}{S_\lambda{}^6}\right)\frac{1}{\beta(\beta\hbar\omega)^4}$$
$$\times e^{-\beta(2\Delta_F-\hbar\omega)}\Big\{1+\beta(2\Delta_F-\hbar\omega)$$
$$+\tfrac{1}{2}\beta^2(2\Delta_F-\hbar\omega)^2+4\beta^3(2\Delta_F-\hbar\omega)^3$$
$$+\beta^4(2\Delta_F-\hbar\omega)^4\Big\}\,, \tag{23}$$

(ii) $2\Delta_F<\hbar\omega<(k_B\theta_D{}^\lambda+2\Delta_F)$(all λ):

$$A(\omega)=\frac{2}{\pi^2}\left(\frac{e^2}{\hbar c}\right)\frac{k_F{}^2}{\hbar^2m^{*2}v_F{}^2\rho_M}\left(\sum_\lambda\frac{C_\lambda{}^2}{S_\lambda{}^6}\right)\frac{1}{\beta^2(\beta\hbar\omega)^4}$$
$$\times\Big\{\frac{5}{4}+\beta(\hbar\omega-2\Delta_F)+\beta\frac{(2\Delta_F)^2}{2\Delta_F+\hbar\omega}$$
$$+\frac{\beta^6}{120}(\hbar\omega-2\Delta_F)^5\frac{(2\Delta_F)^2}{\hbar\omega+2\Delta_F}$$
$$+\frac{\beta^6}{720}(\hbar\omega-2\Delta_F)^6\Big\}\,, \tag{24}$$

(iii) $\hbar\omega>(k_B\theta_D{}^\lambda+2\Delta_F)$(all λ):

$$A(\omega)=\frac{2}{\pi^2}\left(\frac{e^2}{\hbar c}\right)\frac{k_F{}^2}{\hbar^2m^{*2}v_F{}^2\rho_M}\left(\sum_\lambda\frac{C_\lambda{}^2}{S_\lambda{}^6}\right)\frac{1}{\beta^2(\beta\hbar\omega)^3}$$
$$\times\Big\{1+\frac{1}{120}(\beta\hbar q_D)^5\sum_\lambda\frac{C_\lambda{}^2}{S_\lambda}$$
$$\times\left(1-\frac{5}{6}\frac{\omega_D{}^\lambda}{\omega}\right)\Big/\sum_\lambda\left(\frac{C_\lambda{}^2}{S_\lambda{}^6}\right)\Big\}$$
$$:\omega_D{}^\lambda=(k_B\theta_D{}^\lambda/\hbar)\,. \tag{25}$$

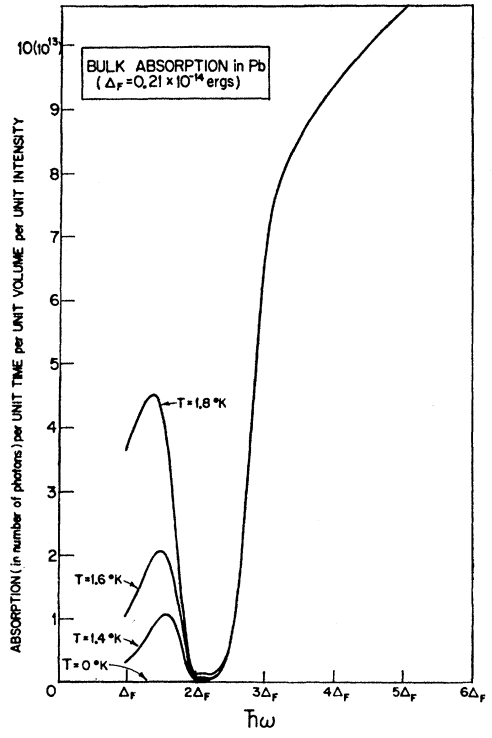

FIG. 3. The spectral shape of the absorption $A(\omega)$ is plotted for ω in the neighborhood of the gap frequency ω_0. Notice the spike very near the gap frequency. Corresponding curve at $T=0$°K is also shown. The spike collapses at $T=0$°K. Note that the value of $A(\omega)$ at $\hbar\omega=5\Delta_F$ is approximately 10 times the value at the peak.

These formulas represent the spectral shape of the absorption in a superconductor.

In order to gain some knowledge on the magnitude as well as the shape of $A(\omega)$ we shall compute it numerically for ω in the neighborhood of the gap frequency for Pb at $T\cong 1.4$°K. Since Pb has a transition temperature T_c of the order of 7°K, the condition $\beta\Delta_F\gg 1$ is met reasonably. We consider Pb here since, being a metal whose normal state conductivity is relatively low compared with some other metals, it is expected to show a relatively large bulk absorption; i.e., Pb has a low Debye temperature. Note that, due to the condition $\beta\Delta_F\gg 1$ for applicability of this formula, we may take

$$\Delta_F(T)\cong\Delta_F{}^0\,,$$

where $\Delta_F{}^0$ is the maximum value corresponding to $T=0$°K. Since we have no knowledge on the magnitudes of $C_\lambda{}^2$, we shall resort to taking an average value $\langle C^2\rangle_{\rm av}$ thus taking it out of the summation over λ. Due to the appearance of the sixth power of S_λ in (23) and (24) and to the fact that the longitudinal phase speed of sound S_L is generally larger than the transverse speed S_T, however, taking

$$\sum_\lambda\left(\frac{C_\lambda{}^2}{S_\lambda{}^6}\right)\approx\langle C^2\rangle_{\rm av}\left(\frac{1}{S_L{}^6}+\frac{2}{S_T{}^6}\right)$$

does not do justice to the longitudinal phonon contributions. For instance, in the case of Pb, it would make the transverse contributions larger than the longitudinal contributions by as much as a factor of 10^2. In general, when $\mathbf{g}=0$, it would be reasonable, even in the case of a relatively complicated lattice, to expect that, at the most, the magnitude of the transverse contributions may not exceed that of the longitudinal contributions. Therefore, there will not be a serious loss in order of magnitude in taking only the longitudinal term such that

$$\sum_{\lambda}\frac{C_\lambda{}^2}{S_\lambda{}^6}\approx\left(\frac{\langle C^2\rangle_{\mathrm{av}}}{S_L{}^6}\right).$$

We shall use this in our numerical calculation. For Pb at 1.44°K, we shall use the following values for various parameters: $\Delta_F=2.1\times10^{-15}$ erg, $k_F=1.6\times10^8$ cm^{-1}, $S_L=2.4\times10^5$ cm/sec, $m=m_0$, $\rho_M=11$ gm/cm^3, $M=3.5\times10^{-22}$ gm, $n_a=1.24$, $\langle C^2\rangle_{\mathrm{av}}=(1.16E_F)^2$, $E_F=\{(\hbar^2/2m^*)(n_a\rho_M/8\pi^2M)^{2/3}\}$. These numerical values are those which were used in Ref. 6 for computing the nonradiative recombination rate.

The spectral shape $A(\omega)$ for $\hbar\omega$ in the neighborhood of $2\Delta_F=\hbar\omega_g$ is computed from the formulas (23) and (24), and is presented in Fig. 3 for three different temperatures.[17] Here, $A(\omega)$ has the dimension of inverse distance per unit energy so that $(A(\omega)\times\hbar\omega)$ has the dimension of inverse distance. It is seen that a spike or an absorption peak is present at a frequency slightly below the gap frequency. The position of the peak varies with temperature. Note also that the spike exhibits a sensitive temperature dependence considering the small temperature range $0°<T<T_c$ that is involved here. At 0°K, it collapses entirely; the absorption vanishes for $\omega<\omega_g$. As the temperature is raised to a value comparable to the transition temperature T_c, the spike may be broadened so much that it would be indistinguishable from the over-all absorption curve.

It may be pointed out that the curves of Fig. 3 bear a resemblance with the curve of the current-voltage characteristics observed in the normal (i.e., not involving radiation) tunneling phenomenon in a superconducting sandwich of metals,[12] the spike of Fig. 3 being equivalent to the negative resistance region in tunneling. This resemblance is not surprising in view of the fact that presence of spikes, in both cases, is attributable to particular properties of the density-of-states function in a superconductor, and in particular, to the large density of states at the gap edges. In fact, this may also account for the peaks observed by Dayem and Martin[9] in their radiative tunneling experiments.

In the present calculations, the physics underlying the appearance of the spike is as follows: at very low temperatures (i.e., $\beta\Delta_F\gg1$), the unpaired band is nearly empty and, likewise, the paired band is nearly filled up so that the absorption at $\omega<\omega_g$ due to the processes (c) and (d) of Fig. 1 is relatively insignificant. On the other hand, a substantial absorption at $\omega<\omega_g$ associated with the intergap transition (a) of Fig. 1 is possible through the inelastic phonon processes in which the energy difference $(\hbar\omega_g-\hbar\omega)$ is compensated by absorption of a phonon quantum. Since the probability for absorption of a phonon is proportional to $N_{\lambda\mathbf{q}}=(e^{\beta\hbar\omega_{\lambda\mathbf{q}}}-1)^{-1}$, the absorption at $\omega<\omega_g$ clearly vanishes at $T=0$°K, and would be significant at $T>0$°K for only small values of the phonon quantum of the order of, say, k_BT. Since the integrand of (17) also contains $(\hbar\omega_{\lambda q})^4$ multiplied to $N_{\lambda\mathbf{q}}$ for the phonon absorption term, $A(\omega)$ has a minimum at $\omega=\omega_g$. For these reasons, the peak appears at a frequency slightly below the gap frequency ω_g. Further, since the large value of the density of states at the gap edges makes the edge-to-edge transitions most favorable, the spike would appear at a frequency which corresponds to $(\omega_g-\langle\omega_q\rangle)$, $\langle\omega_q\rangle$ being the average phonon quantum which participate in the processes in consideration at a given temperature.

It may be noted that the sharpness and the sensitivity to temperature of the spike are largely attributed to the sharpness (i.e., the singularity) of the BCS density-of-state function at the gap edges. For real superconductors, however, one should use an appropriate cutoff density-of-state function, thus removing the singularity at the edges.[13] This might effect in making the spike less sensitive to temperature and less sharp than what has resulted in the present calculations. Further, the position of the peak would be also affected by the cutoff.

As T is increased in the range $0<T<T_c$, the position of the peak would shift to lower frequencies since $\langle\omega_q\rangle$ increases and the energy gap shrinks with increase in temperature. At the same time, the spike would be gradually smeared since the absorptions associated with the processes (c) and (d) of Fig. 1, for example, become more important at higher temperatures.

It may be reminded here that the results of the present calculations are not capable of showing the complete behavior of the spike for the entire temperature range, $0<T<T_c$ since we have assumed $\beta\hbar\omega$, $\beta\Delta_F\gg1$.

In order to obtain a comparative order of magnitude of the bulk absorption, we may calculate some typical values of the power absorbed per unit volume W in W/cm^3. In terms of $A(\omega)$, W is given by

$$W=\{(A(\omega)\times\hbar\omega)(\mathrm{cm}^{-1})xI_0(\mathrm{W/cm}^2)\},$$

where I_0(W/cm^2) is the intensity of the incident radiation. At the absorption maxima, we have $A=1\sim5\times10^{13}$ for $T=1.4\sim1.8$°K as shown in Fig. 3. This corresponds to

$$W\approx(0.03\sim0.2)\times I_0(\mathrm{W/cm}^3).$$

For a penetration depth $\delta\approx400$ Å, this represents an

[17] The author thanks Dr. A. J. Freeman for the help rendered with the numerical computations.

absorptivity of

$$(A(\omega)\times\hbar\omega\times\delta)\approx 10^{-7}\sim 10^{-6}$$

at the spike frequencies, and is smaller, for example, by a factor of $10^4\sim 10^3$ than the absorptivity of 2.5×10^{-3} in the normal state Pb at ω_g measured by Richards and Tinkham.[4] At ω substantially larger than Δ_F, the ratio of $A(\omega)$ relative to that at ω_g is given by

$$\frac{A(\omega)}{A(\omega_g)}\approx\frac{1}{45}(\beta\Delta_F)^5\left(\frac{\hbar\omega}{\Delta_F}\right)^2$$

for $\hbar\omega<k_B\theta_D$. Using $A(\omega_g)\approx 2\times 10^9$ at $T=1.4°\mathrm{K}$ which is calculated from the formula,

$$A(\omega_g)=\frac{(e^2/\hbar c)k_F^2(k_BT)^6}{8\pi^2\hbar^2(m^*v_F)^2\rho_M(\Delta_F)^3}\sum_\lambda\frac{C_\lambda^2}{S_\lambda^2},$$

we obtain $A\approx 1\times 10^{14}$ at $\hbar\omega=5\Delta_F$ and $T=1.4°\mathrm{K}$, which is approximately 10 times the value at the spike maximum.

While all these suggest, beyond any doubt, that the bulk absorption is too small to explain the observed absorption and hence is likely to be insignificant compared with the skin absorption as far as the order of magnitude is concerned, the fact that the bulk mechanism considered here gives rise to an absorption peak at $\omega<\omega_g$ which is not found in the skin absorption[7,8] may have some practical significance.

The experimental evidence for the presence of the spike may be found in the observations of Richards and Tinkham[4] and Richards[10] which show a structure suggestive of the spike that has been obtained here. These authors present the curves for (P_S-P_N/P_N) which represents the power absorption of superconductor (P_S) relative to that of the normal metal (P_N) at the same temperature. In their curves, the spike of the present paper corresponds to a dip since the normal metal should exhibit a larger absorption than the superconductor of same temperature due to its residual absorptivity (and hence residual resistance) at very low temperatures: see Refs. 1–3. In the measurements of Richards and Tinkham[4] on Pb and Hg, the structure appears to be an absorption peak at $\omega<\omega_g$, thus in agreement with the present result. On the other hand, while Richard's curves on Sn appear to have spectral shapes which resemble what is given by the present theory, they appear to suggest absorption maxima above the gap frequency ω_g. In this case, therefore, the present theory does not fare well with the experiment.

Finally, it is important to note that we have considered only the non-umklapp processes here, and that neglecting the umklapp contributions is not always justified since the relative importance of the umklapp processes varies not only with the materials in consideration, but also with temperature; e.g., at very low temperatures where only the very low-energy phonons contribute significantly, the umklapp contributions can be quite substantial in some metals since q^4 multiplying $N_{\lambda\mathbf{q}}$ and $(1+N_{\lambda\mathbf{q}})$ in the integrand of (17) would then be replaced by $K^4=(\mathbf{q}+\mathbf{g})^4\approx g^4$. This would clearly shift the spike toward the gap frequency ω_g, the magnitude of the shift being determined by the "nearest-neighbor" values of the reciprocal lattice vector $\mathbf{g}$. The umklapp contribution to the bulk absorption in superconducting Pb and Sn will be the topic for a future publication.

ACKNOWLEDGMENTS

The author gratefully acknowledges profitable discussions with Dr. Benjamin Lax and with Dr. M. Tinkham whose constructive criticism has been essential in shaping the revised version of the manuscript. He also thanks Dr. P. Argyres for reading the manuscript and Dr. A. J. Freeman for his continued encouragement and for the help rendered with numerical computations.